Rotor–Stator Rubbing Contact in an Overhung Rotordynamic System

1 author:

Philip Varney
Georgia Institute of Technology
15 PUBLICATIONS **128** CITATIONS

Rotor-Stator Rubbing Contact in an Overhung Rotordynamic System

Phil Varney (pvarney3@gatech.edu)
Georgia Institute of Technology
801 Ferst Drive, Atlanta, GA 30332

Itzhak Green (itzhak.green@me.gatech.edu)
Georgia Institute of Technology
801 Ferst Drive, Atlanta, GA 30332

Introduction

Increases in turbomachine efficiency are often achieved via higher operating speeds, increased shaft flexibility, and decreased fluid film clearances. Unfortunately, these changes increase susceptibility to faults such as rotor-stator rubbing contact. Rubbing contact between the rotor and stator results in decreased machine life via increased wear, heightened susceptibility to fatigue, and adverse thermal effects. Preventing rub requires detailed knowledge of the coupled rotordynamic-triboelement dynamic conditions. Beatty [1] and Lee and Green [2] indicate the presence of higher harmonic oscillations in the rotor response through a simple qualitative model of rub. Rotor-stator rubbing is an inherently nonlinear phenomena, resulting in a rich nonlinear dynamic response including periodic, quasiperiodic, and chaotic vibrations. Chaotic phenomena in rotor systems undergoing rub are discussed by Chu and Zhang [3]; this work and others [4, 5] also highlight other nonlinear phenomena, such as subharmonic frequencies, periodic responses, and quasiperiodic responses. Qin et al. [6] provide an initial investigation into an overhung rotor, focusing of grazing bifurcations and routes to chaos induced by lateral rub. This work advances the state-of-the-art in dynamic rotor-stator rubbing contact by providing closed-form, analytical equations of motion for a gyroscopic overhung rotor including both lateral and angular rub to simulate dynamic contact of the rotor with a mechanical face seal. Contact force expressions are developed along with conditions for contact, and the equations of motion are solved numerically. Periodic, quasiperiodic, and chaotic phenomena are observed using rotor orbits, Poincare maps, frequency spectra, and bifurcation diagrams. Routes to chaos are discussed, along with the influence of clearance and friction.

Modeling

The overhung rotordynamic system is shown in Fig. 1, along with the inertial reference frame XYZ. The lateral, or annular, contact is modeled using the Coulomb friction – elastic contact model employed by many authors [1, 3, 5, 8, 9], where contact results in an elastic normal restoring force and tangential friction force. The equations of motions including displacements (u_x, u_y) and tilts (γ_x, γ_y) of the rotor in the inertial frame are [7]:

Figure 1: Overhung rotordynamic system

$$[M]\{\ddot{q}\} + ([D] + [G])\{\dot{q}\} + [K]\{q\} = \{F\} \qquad \text{Eq. 1}$$

where $\{q\}$ represents the state vector and $\{F\}$ the vector of forces including imbalance, gravity, and, added here for the first time, contact. The lateral clearance of the rotor is δ, the rotor's radial position is r, the contact stiffness is k_c, and the friction coefficient is μ. Figures 2 and 3 demonstrate the rotor's angular, or face, contact with a hypothetical obstruction such as a mechanical face seal. The clearance between the rotor's face and the seal is designated δ_a, the contact stiffness is k_{ca}, friction coefficient μ_a, and the single radial value at which contact is permitted is r_p (assumed from this point to be the rotor's radius, R). The deflection of a point on the rotor in the z-direction is designated r_z. It is assumed that the contact force acts through the centroid of the contact line, which is determined by the location at which r_z is the greatest; the angular position of this location is designated by angle θ_c.
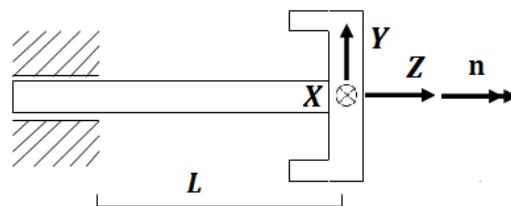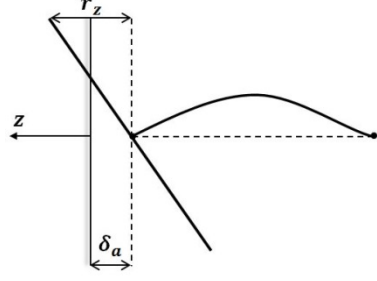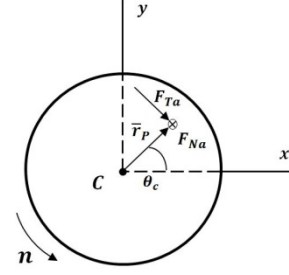
Figure 2: Angular contact forces

Figure 3: Angular face contact clearances

The complete forcing function, including imbalance, gravity, and lateral/angular contact forces is

$$\{F\} = \begin{Bmatrix} m\epsilon n^2 \cos(nt) \\ m\epsilon n^2 \sin(nt) - mg \\ 0 \\ 0 \end{Bmatrix} + \phi_L \begin{Bmatrix} \mu u_y - u_x \\ -(\mu u_x + u_y) \\ 0 \\ 0 \end{Bmatrix} + \phi_a \begin{Bmatrix} \mu_a \sin\theta_c \\ -\mu_a \cos\theta_c \\ -r_p \sin\theta_c \\ r_p \cos\theta_c \end{Bmatrix} \qquad \text{Eq. 2}$$

$$\phi_L = k_c \frac{r - \delta}{r} h(r - \delta), \qquad \phi_a = k_{ca}(r_z - \delta_a)h(r_z - \delta_a)$$

where ϵ is the rotor eccentricity, m is the rotor mass, and n is the shaft speed. Inclusion of gravity is imperative due to the nonlinearity of the equations: the resulting motion is no longer the superposition of the static response due to gravity and the dynamic response. The intermittency of contact generates a strong system nonlinearity, represented above via the Heaviside function $h(x)$, which is unity when x is positive and zero when x is negative.

Results

The equations of motion are non-dimensionalized in time and solved numerically using a hybrid $4^{th}/5^{th}$ order Runge Kutta integration scheme. Figure 4 demonstrates a period-3 orbit, as evidenced by three distinct points in the Poincare section (obtained via a stroboscopic picture of the response at the non-dimensional time interval 2π). Only the tilts are shown, as the lateral response is qualitatively identical. A quasiperiodic (QP) orbit on a two-torus is shown in Fig. 4, where the QP motion is evidenced by closed curves on the Poincare section and incommensurate frequencies in the frequency spectra. Chaotic motion is seen in Fig. 6, as evidenced by a seemingly random Poincare section and broadband frequency content.
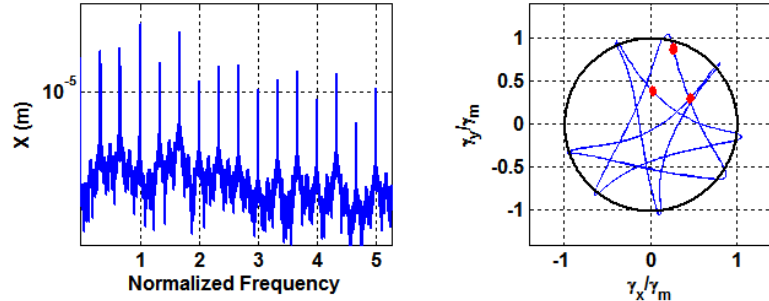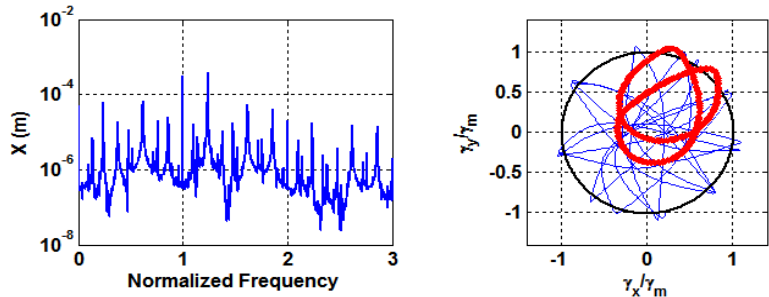

Figure 4: Period-3 motion at n = 230 rad/s

Figure 5: Quasiperiodic motion at n = 300 rad/s

Such richly varied responses can be found for many shaft speeds and parameter combinations. A typical route to chaos, period doubling bifurcation, is shown in Fig. 5.

A parametric investigation into the lateral clearance δ reveals that decreasing the clearance results in a bifurcation from periodic to quasiperiodic to chaotic response.

Figure 6: Chaotic motion at n = 330 rad/s

Likewise, increasing the friction coefficient leads to the eventual appearance of chaotic behavior. Such analysis could be performed for many system properties, such as shaft stiffness, contact stiffness, damping, eccentricity, etc. Such an analysis is beyond the introductory scope of this work.

Several important conclusions can be drawn from the results. First, the qualitative nature of the response strongly depends on many possible parameters. Appropriately choosing this parameters is essential for obtained realistic results. Second, the angular and lateral motion are qualitatively similar. Thus, for example, conclusions can be drawn concerning the rotor's lateral motion even if the monitoring system only measures the rotor's angular response. To fully model rotor contact with a mechanical face seal, however, the full fluid film and misalignment effects must be incorporated: this task is reserved for future work.
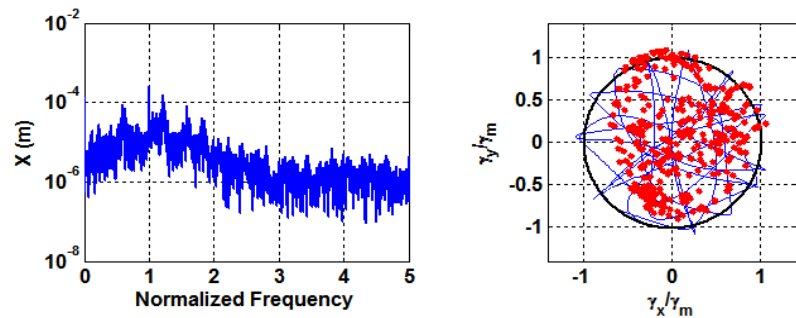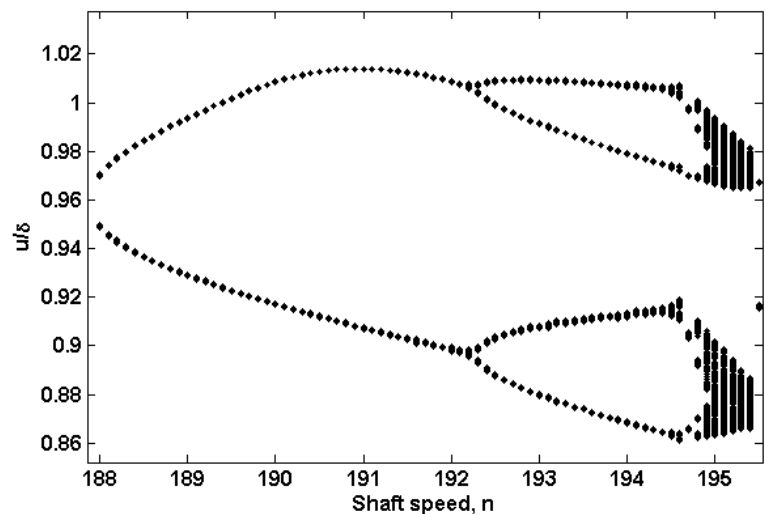

Figure 7: Period doubling evident from the bifurcation plot

References

[1] Beatty, R. F. *Differentiating Rotor Response Due to Radial Rubbing*. Journal of Vibration, Acoustics, Stress, and Reliability in Design, **107** (1985), p. 151 – 160.

[2] Lee, A. S. and Green, I. *Higher Harmonic Oscillations in a Non-contacting FMR Mechanical Face Seal Test Rig*. Journal of Vibration and Acoustics, **116** (1994), p. 161 – 167.

[3] Chu, F. and Zhang, Z. *Bifurcation and Chaos in a Rub-Impact Jeffcott Rotor System*. Journal of Sound and Vibration, **210**(1) (1997), p. 1 – 18.

[4] Chang-Jian, C. W. and Chen, C. K. *Chaos and Bifurcation of a Flexible Rub-Impact Rotor Supported by Oil Film Bearings with Nonlinear Suspension*. Mechanism and Machine Theory, **42** (2007), p. 312–333.

[5] Inayat-Hussain, J. I. *Bifurcations in the Response of a Jeffcott Rotor with Rotor-to-Stator Rub*. ASME 10th Biennial Conference on Engineering Systems Design and Analysis, (2010), p. 1 – 10.

[6] Qin, W. and Chen, G. and Meng, G. *Nonlinear Responses of a Rub-Impact Overhung Rotor*. Chaos, Solitons, and Fractals, **19**(5) (2004), p. 1161 – 1172.

[7] Varney, P. *Transverse Fatigue Crack Diagnosis in a Rotordynamic System Using Vibration Monitoring*. Master's Thesis, Georgia Institute of Technology, **2013.**